ORIGINAL RESEARCH PAPER

Volume - 10 | Issue - 08 | August - 2021 | PRINT ISSN No. 2277 - 8179 | DOI : 10.36106/ijsr

INTERNATIONAL JOURNAL OF SCIENTIFIC RESEARCH

# A STUDY OF SURFACE AREA CLASSIFICATION OF BHIWANI AREA USING SENTINEL-1 SAR IMAGES

Computer Science

**Prachi Kaushik*** Research Scholar, Department of Computer Science, Jamia Millia Islamia, New Delhi. *Corresponding Author

**Dr. Suraiya Jabin** Professor, Department of Computer Science, Jamia Millia Islamia, New Delhi.

## ABSTRACT

Synthetic Aperture Radar (SAR), an active radar system which helps in formation of high-resolution images capable of sea and land monitoring, soil moisture monitoring, and disaster response monitoring. The quality of the image is degraded by grainy speckle noise, so it becomes necessary to pre-process the images before any kind of analysis. This paper gives a detailed description of effective pre-processing steps such as orbit file correction, calibration, speckle filtering, radiometric terrain correction for C-band Sentinel-1 Level-1 GRD (Ground Range Detected) SAR images. We have applied classification algorithms to the raw and pre-processed images to classify them into different categories such as agricultural land, urban areas, trees, and water bodies. The experimental results demonstrate that there is a significant improvement of 15% and 13.1% in the classification accuracy of an image after applying the pre-processing steps for the K-Nearest Neighbour and Random Forest algorithms. The lesser explored pre-processing step orbit file correction further improves the overall accuracy by 1.52% according to the experimental analysis.

## KEYWORDS

Sentinel-1, pre-processing, Random Forest, Orbit file, SAR.

## 1. INTRODUCTION

In the last few decades, new and more advanced technology of remote sensing has come up to monitor the earth's environment and ecosystem so far in more accurate way by the use of satellites orbiting the earth's surface such as SAR (Synthetic Aperture Radar). SAR has an active sensor that produces high resolution quality images of the earth's surface by the use of large synthetic aperture antenna. These images are created by sending the radio signals from the active radar to the area being scanned and the reflected signals are captured by the sensors **[1]**.

Sentinel-1 is the first important synthetic aperture radar mission operating at a frequency of 4-8 GHz and 3.8-7.5 cm wavelength. It has an aim to continuously map the earth's surface to provide enhanced revisit time, which makes it suitable for marine, land, climate change and emergency response monitoring. This RADAR has a capability to capture images in day and night as well as to see through clouds in the conditions of rain. SAR images are valuable resource to monitor tropical areas with frequent cloud cover.

In conditions of flood, it helps to speed up the response initiatives, evacuation plan, and assess damage over the affected area. A very useful application of SAR data is to monitor the ice and glaciers on high altitudes based on the backscatter values deriving information on ice type and its concentration.

On the Ocean surface, illegal or accidental oil spills are easily visible and can be identified with the radar imagery. Another useful application is to map the deformations and movement of few centimetres in the earth surface due to earthquakes and landslides, which is made possible by interferometry SAR (In-SAR) technique.

The process of SAR image formation is affected by thermal noise, speckle noise, border noise, calibration and radiometric terrain errors. The granular interference of the backscatter from the non-uniform cells creates a grainy speckle noise affecting the quality of image. The accuracy of the classification is enhanced by removing the errors due to geometry and intensity of pixels in the image at each pre-processing step to extract useable information **[2]**.

The flowchart in figure 1 describes the flow of steps to analyse the importance of the pre-processing workflow for SAR image classification. Sentinel-1 Band-C SAR image and optical sentinel-2 images are acquired for this study. A high-quality training dataset for the region of interest (ROI) is prepared to train supervised classifiers from the false colour composite (FCC) of the sentinel-2 image. Supervised classifiers like Random Forest (RF), Maximum Likelihood (ML), and K-Nearest Neighbour (KNN) classify original (Raw) terrain corrected and pre-processed Sentinel-1 images.

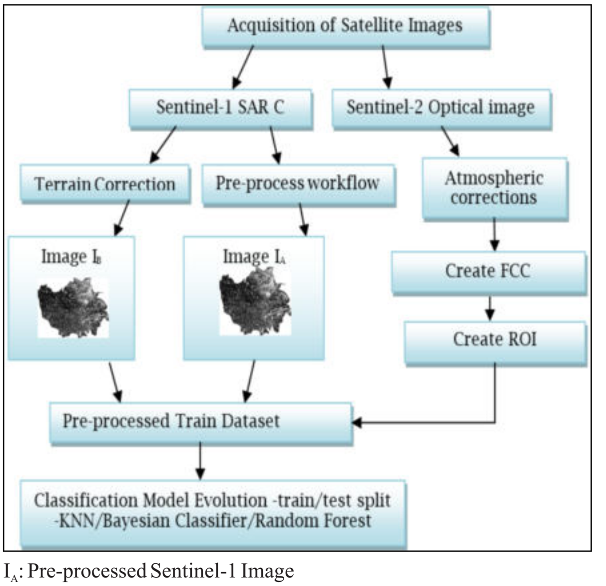


$I_A$: Pre-processed Sentinel-1 Image
$I_B$: Level-1 GRD Sentinel-1 Image
(Without pre-processing)

**Fig.1. Flow Diagram for Land cover classification of Bhiwani District, Haryana, India.**

## 2. Literature Review: State of the art Pre-processing and Classification techniques for Sentinel-1 images

Sentinel-1 Active Radar SAR satellite dual polarization data offers an effective classification into land cover classes over the single band images. The acquired image data needs to be pre-processed to extract the key features for the classification studies. There have been many studies which focus on the filtering of the grainy noise in the image to improve the accuracy of classification. This section gives an overview of the pre-processing techniques, review of most prevalent SAR pre-processing techniques for effective classification, and review of classification techniques for Land Use and Land Cover mapping.

### *A. Pre-processing techniques overview*

The SAR data gathered by the SAR sensors often lead to distorted images not suitable for image classification and segmentation. This data is cleaned, transformed, reduced and transformed for mining the actionable information from satellite data. Before applying any analysis, the quality of the data is given prime importance by filtering the noise as discussed below.

#### *i. Speckle filtering*

While image acquisition of SAR imagery, by coherent de-modulation of reflected electromagnetic waves, multiplicative/periodic/speckle noise is inherently added to the images. Lukin et al. [**3**] have stated that speckle in Sentinel-1 SAR image is pure multiplicative noise with the variance approximately 0.05. The speckle is spatially correlated and practically independent for VV and VH bands with cross-correlation factor of 0.8. Hence speckle noise removal is an important pre-processing step before using SAR images for any kind of analysis. The basic idea is that periodic noise appears as concentrated bursts of energy in Fourier transform of acquired image, at locations corresponding to frequencies of periodic interference. The solution is to use a selective filter e.g., notch reject filter to isolate the noise.

There are two broad classifications of speckle filters, adaptive filters and non-adaptive filters. The adaptive filters have the ability to accommodate the changes in the local properties of the terrain backscatter. It preserves the edge and the texture information in the image. The Non-adaptive filters take the whole image as the parameter to the filtering step. This filtering is simple to implement and requires lesser computational resources **[4][25]**. Table 1 gives the properties of common speckle filters implemented in the GIS software which can be directly applied on the image, setting the window size(3x3, 5x5, 7x7, 11x11 etc.) and threshold values.

**Table1. Properties of Filters**

| Filter | Properties |
|---|---|
| Boxcar (Mean) | Non-linear filter, reduces detail and resolution<br>value (centre pixel) = mean (neighboring pixel) |
| Median | Non-linear filter, reduces detail and resolution<br>value (centre pixel) = median (neighboring pixel) |
| Frost | Exponentially damped circularly symmetric linear filter<br>Uses coefficient of variation within filter windows [5]<br>Preserves the edge information |
| Gamma Map | Gamma Distribution for texture modeling<br>Maximum Likelihood estimation to extract detected intensity<br>Window size 7x7 best for crop classification |
| Lee | Spatial filter applied to each pixel in image<br>calculation of local statistics within the square window<br>value (centre pixel) = calculated value (neighboring pixel) |
| Refined Lee | Preserves image sharpness, detail, point target and texture information |
| Lee Sigma | Based on Gaussian distribution model<br>Averages pixels under certain standard deviation |
| Intensity Driven Adaptive Neighborhood (IDAN) | Adaptive filter<br>pixel neighborhood formed using region growing method<br>selected pixels are not required to lie within a fixed moving window |

Most of the authors like Nyoungui et al. [**6**], Mansourpour et al. [**7**] have focused on the speckle noise removal in SAR data and comparison of different speckle filters such as Lee, frost, gamma map filters with window size of 5x5 which show better results due to low standard deviation. Lee and frost filters can be reasonable choices in visual interpretation of the image as it can preserve the edges, texture information, point target information, etc.

***ii. Frequency and Wavelet Domain Filtering***

An important filtering for smoothing and sharpening of SAR image edges is done by frequency domain filtering. The Fast Fourier transform computes the frequency components by decomposition of input images into Sine and Cosine values which are basis of various spectral estimation algorithms. In frequency domain filtering, first the input image is transformed using a transform like Sine, Cosine, Fourier, etc. After performing the specific task by applying a filter in frequency domain, an inverse transform is applied to return to the spatial domain.

A number of papers [**8**][**9**][**10**][**11**] have used frequency domain SAR image processing for their specific tasks. It is a non-parametric method for estimating the spectral measurements after the application of Discrete Fourier transform making the process suitable for time independent analysis.

Edge is the most valuable information in the image which can be extracted as shape feature in feature vector. To preserve this information only noise is filtered in this step. In Discrete wavelet transform, each section of the wavelet is measured w.r.t. correlation with each section of the signal to improve the filtering. The wavelet transform outperforms the Fast Fourier transform.

***B. Review of Pre-processing techniques***

LiAining [**8**] explained the 2D processing of azimuth and range compression to propose a new algorithm. This is based on the principal of stationary phase and frequency domain features for X-band SAR images using the Taylor series. The frequency domain SAR processing algorithms are inadequate to handle lower central frequencies, high bandwidth and wide beam widths [9].

A generalized algorithm integrating Radar-Doppler algorithm and chirp scaling algorithm has been proposed by E.C. Zaugg [9] to extend the frequency domain filtering and processing. Ranjitha & Hiremath [10] proposed a new technique of DWT-SVM-NN to remove impulsive noise in the satellite images. This technique efficiently increased the Peak signal-to-noise ratio (PSNR) and the structural similarity index with fast computational speed. Y. Gao et al. [11] gave a method for phase filtering using amended matrix pencil and linear window mean filter. It outperformed in areas with high fringe density and low coherence for In-SAR processing.

The local frequency is calculated with amended pencil matrix algorithm highlighting the topographic changes. These frequencies are filtered by the linear window mean filter thus improving the quality of the image.

***C. Review of SAR Classification techniques***

Several studies in literature have focused on analyzing the potential of Sentinel-1 cloud free images in conditions of flood mapping and change detection using histogram threshold, supervised and unsupervised algorithms, and change detection through time series data.

Abdikan et al. [12] exploited different combinations of VV and VH bands to create accurate land cover maps implementing supervised SVM classification. Adding difference of the two bands (VV-VH) as the third variable achieved 93.28% classification accuracy. Tavares et al. [5] have shown that integration of Sentinel-1 and Sentinel-2 optical images have presented better results of 91.07% accuracy with random forests for LULC mapping in tropical regions rather than S-1 or S-2 images. Fonteh et al. [13] compared and fused cloud free Landsat [24] and Sentinel-1 images for land cover classification using Support Vector machine (SVM). Based on the experiments, Landsat spectral bands (5,6,7) proved to be the best with an accuracy of 91.96% in LULC studies as compared to Sentinel-1 VV, VH bands.

SB Bohra et al. [14] classified the SAR image into water and non-water class based on the unsupervised K-means clustering as the ground truth information was not available during flood event. Amitrano et al. [15] proposed two level flood detection technique by extracting the co-occurrence texture measures for fuzzy classification in level 1 and change detection in level 2. Chang Lie [16] used time series analysis of Sentinel-1 images to detect standing water based on backscatter temporal variability. Twele et al. [17] monitored the floods in real time by automatic Sentinel-S1 processing chain. This chain has the capability to give disaster information within 45 min. of the disaster event. G. Boni et al. [18] proposed a flood forecast system combining COSMO-SkyMed and Sentinel-1 satellite for flood monitoring.

We can conclude that the most frequently used pre-processing techniques of SAR images for a variety of applications are calibration, speckle filtering, and terrain correction. However, the step of orbit correction has not been explored as a pre-processing step very frequently for land surface classification. With this literature review, we explore the importance of pre-processing steps to map exact geographical coordinates of the image on the ground for geo-coding enhancing image accuracy.

The study of the classification techniques suggests that the fusion of SAR and optical images have shown tremendous improvement in the classification accuracy as compared to only SAR images. In the purview of these conclusions, we prepare a pre-processing workflow and apply it before classification of surface area for the proposed work.

 PRINT ISSN No. 2277 - 8179 | DOI : 10.36106/ijsr

## 3. MATERIALS AND METHODS

In this section we describe area of study, data extraction, ROI, and pre-processing workflow, and application of classification methods.

### *A. Area of Study*

In this classification study, Sentinel-1A Ground Range Detected (GRD) Level-1 product of Haryana state covering Bhiwani district with 28.7752° N latitude and 75.9928° E longitude district shown in Figure 2 was downloaded from SCIHUB [19]. The image having dual polarization (VV+VH) and acquisition mode interferometric Wide swath (IW) was taken for the date of 18th November 2019.

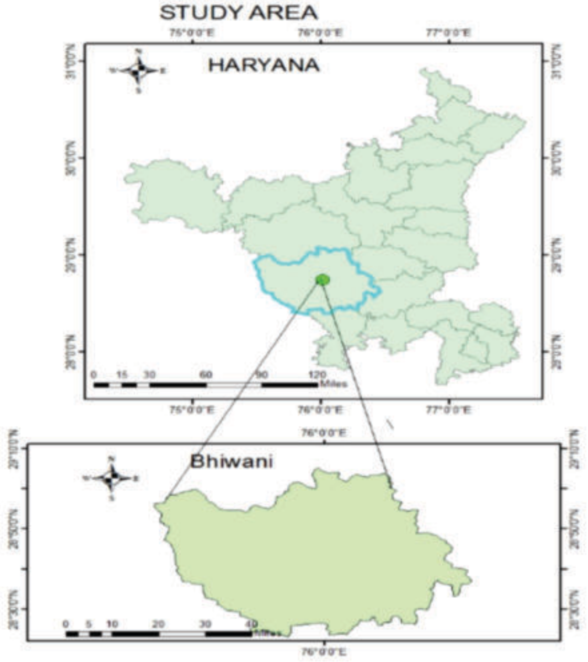


**Fig.2. Study Area of Bhiwani District, Haryana, India**

### *B. Source of Data and Extraction Steps*

Data Acquisition is the initial and the most important step for different classification studies. The data can be downloaded from Copernicus Open Access Hub [19] after registration and login into the portal after signing terms and conditions [20]. The study area of Bhiwani district is selected by navigating around the world map to the state of Haryana and drawing rectangle or polygon for the interest area. For the purpose of this study band C sentinel-1 satellite data product with acquisition mode of Interferometric Wide swath (IW) and Level-1 GRD (Ground Range Detected) having dual bands (VV+VH) is selected. Another data product for the same area is downloaded for sentinel-2 satellite with a spatial resolution of 10m to 60 m operating in 13 multi-spectral bands making it suitable for land cover classification.

Table 2 lists the data products for two satellites Sentinel-1(SAR) and Sentinel-2(Optical) which are loaded into SNAP (*Sentinel Application Platform*) (version 6) [21] for extraction process. The SNAP is an open-source toolbox developed by European Space Agency which has a wide collection of processing, classification, analysis tools for sentinel data products.

**Table2. Image Dataset used in the present Classification Study**

| Satellite Image | Data product | Bands | Type | Date |
|---|---|---|---|---|
| Sentinel -1 | S1A_IW_GRDH_1SDV_20191118T005211_20191118T005236_029958_036B51_AB26 | VV, VH | SAR Band C | 18/11/2019 |
| Sentinel -2 | S2A_MSIL2A_20191119T054121_N0213_R005_T43REM_20191119T075706 | B2, B3, B4, B5, B6, B7, B8, B8A, B11, B12 | Optical | 19/11/2019 |

### *C. Pre-processing Workflow*

This section explains the pre-processing steps taken for the Sentinel-1 images before applying any classification techniques also shown in figure 3.

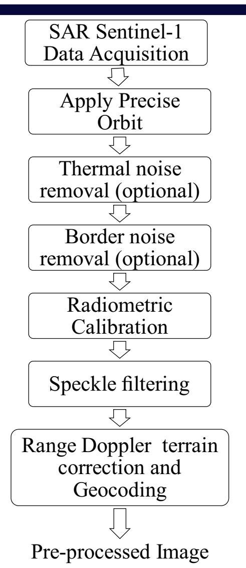


**Fig. 3. Pre-processing workflow for Sentinel-1 Images**

#### *i. Apply Orbit File*

The satellite position and the velocity information are recorded by the global navigation system (GNS) during the image acquisition. The orbit vector values calculated by the on-board navigation facility are added in the product metadata for the Sentinel-1 data product. These orbit vectors do not provide accurate information about the position and velocity of satellite. The orbit information is refined by Copernicus precise orbit determination (POD) service in the form of precise or restituted orbit files. The restituted orbit files are available after 3 hours of data acquisition but precise orbit file is only available after 20 days. Relationship between the ground and the image coordinates is defined in this pre-processing step to improve geo-coding.

#### *ii. Radiometric Calibration*

Radiometric calibration is a conversion step to transform the pixel values from Digital Number ($DN_i$) to corresponding radar backscatter using calibration coefficient included within the SAR products. The radar backscatter coefficient Beta(θ) is only dependent on the DN values of image and not on the local incidence angle of pixels. Sigma(θ) is defined as per unit area on the ground. This coefficient is independent of geometric effects and dependent on the local incidence angle of pixels. Gamma(θ) backscatter coefficient returns radar reflectivity per unit area in plane perpendicular to direction of measurement.

#### *iii. Speckle Filtering*

Noise signals in radar imagery is a result of variable backscatter from uneven and rough earth surfaces modifying the texture and the spectral signatures of roads, urban areas, agricultural lands and water bodies. The radio signals sent from the active radar system on the earth surface is modelled as a function of scattered signals which interfere with the non-uniform cells adding to the dotted or grainy appearance in the image. One of the most important steps is to remove this speckle noise from the images selecting the appropriate filter with correct window size and threshold factor using the available tools. The step of speckle filtering is experimentally tested for varying window size (3X3, 5X5, 7X7). The Lee filter [7] is a spatial filter based on calculation of local statistics within the square window. The filter with window size of 5x5 shows better results as the difference between the means of original and filtered image is less along with low standard deviation.

#### *iv. Terrain Correction and Geo-Coding*

Digital elevation model (DEM) [22] is a digital representation of land surface elevation to remove geometry/topography dependent distortions to normalize measured backscatter with respect to terrain slope. It removes foreshortening, layover, shadow and converting it to a geographic coordinate system. Data from Shuttle Radar Topography Mission (SRTM) with a resolution of 1-arc sec (30m) is used for the DEM (automatic download) or SRTM 3-arc (90m) for map projection. It makes use of orbit state vectors information in metadata, radar timing annotation, slant to ground range conversation parameters, and reference DEM to derive precise geo-location of each pixel.

PRINT ISSN No. 2277 - 8179 | DOI : 10.36106/ijsr

### *D. Extracting ROI for dataset formation*

The region of interest (ROI) extraction takes the advantage from the optical imagery. A Sentinel-2 image for the date of 19/11/2019 is downloaded and pre-processed for atmospheric corrections and cloud masking. The MSI instrument mounted on this satellite covers 13 spectral bands out of which combination of only 10 bands (B2, B3, B4, B5, B6, B7, B8, B8A, B11, B12) are required here. False color infrared (8-4-3) FCC is the most useful combination to extract the region of interests as the dense vegetation reflects the near infrared band due to high chlorophyll content. Urban areas are shown as white and water bodies appear black in colour. Polygons for each land cover class is stored as shape files from the Sentinel-2 FCC image to train the classification algorithms.

## 4. Experiments and Results

The aim of this study is to analyze the improvement in the land surface classification accuracy of an area after applying proposed pre-processing workflow on the Sentinel-1 images.

### *A. Test dataset and Accuracy Assessment*

Assessment points or test samples are randomly selected as the ground truth points from the base map. A total of 168 assessment points is collected over the area of interest covering all the land cover classes. These points are mapped to the classified results to compute the confusion matrix. The accuracy is calculated by dividing the true positives with the total number of test points.

### *B. Classification Results*

The Figure 4 and Table 3 show the accuracy of different classification approaches before and after pre-processing.

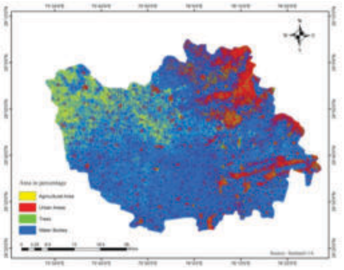

**(a) Random Forest (before pre-processing)**

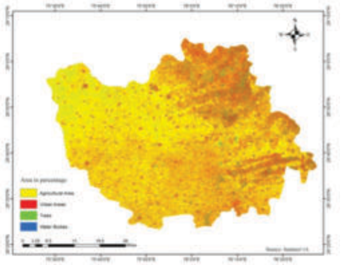

**(b) Random Forest (after pre-processing)**

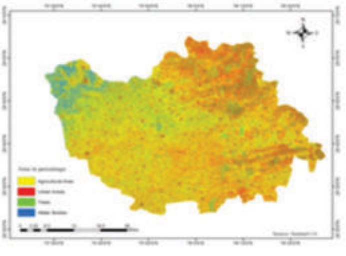

**(c) Maximum likelihood (before pre-processing)**

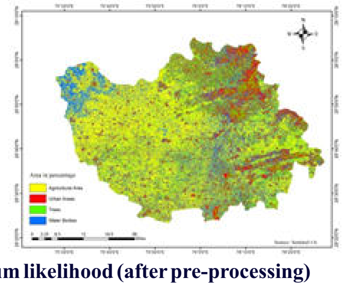

**(d) Maximum likelihood (after pre-processing)**

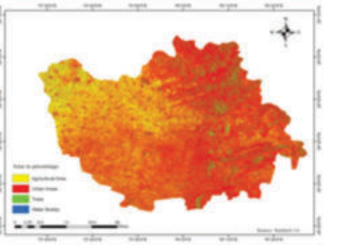

**(e) KNN (before pre-processing)**

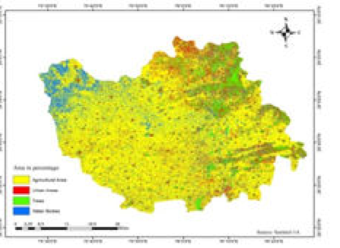

**(f) KNN (after pre-processing)**

**Fig.4. Classification results of Random forest, Maximum likelihood, KNN**

The accuracy assessment in Table 3 clearly shows the improvement in the classification accuracy results after image pre-processing. Most of the pre-processing measures improve the quality of the image (geo-location, speckle noise) which sometimes may not be directly visible. Calibration is good to remove the impact of the incidence angles so that the pixels in near and far range are classified to the correct class. In this study, out of the experimented classifiers, only maximum likelihood algorithm did not show a significant increase (1.03%) in the accuracy of classification after pre-processing.

**Table 3. Accuracy Assessment**

| Classification Algorithm | Accuracy IB (Original image with Terrain Correction) | Accuracy IA (Pre-processed Image) | Increase in Accuracy |
|---|---|---|---|
| Random Forest | 49.4% | 62.5% | +13.04% |
| Maximum Likelihood | 67.2% | 68.23% | +1.03% |
| K-Nearest Neighbor | 57.7% | 73% | +15% |

Based on the literature review the step of orbit file correction has not been explored from the pre-processing chain. So, in order to especially study the effect of this step, the raw and the image pre-processed with orbit file correction are classified with KNN algorithm. The 30 random points are evaluated for any change on the pixel level which are validated from Google earth engine. These 30 pixels are added to the 168 test points for calculation of the accuracy for orbit file correction. A detailed analysis was done at the pixel level to observe the pixel changes after the orbit file correction step. Initially the KNN classifier predicted 17 pixels with correct class labels. However, we obtained that 4 pixels changed their class labels from water body to agricultural land. 2 pixels which were earlier categorised as urban area changed its label to agricultural land. 3 pixels changed from urban areas to trees and 2 pixels from trees to urban areas but 9 pixels remain unchanged counting to a total of 20 pixels. Table 4 shows the percentage increase of 1.52% in the overall accuracy after orbit file correction in case of KNN classifier using the pixel change at low level.

**Table 4. Experimental Analysis of orbit File Correction Step**

| Parameter | Before Orbit file Correction | After Orbit file Correction |
|---|---|---|
| No. of Test pixels | 30 | 30 |
| No. of pixels with correct labels | 17 | 20 |
| Overall Accuracy | 57.57% | 59.09% |
| Observation in terms of increase in Accuracy | **+1.52%** | |

KNN and random forest classifiers both show a significant improvement of around 15% and 13.1% respectively after applying the proposed pre-processing steps. Hence for the Sentinel-1, satellite image pre-processing is an essential step to improve the accuracy of classification, change detection, segmentation, or any particular analysis.

 PRINT ISSN No. 2277 - 8179 | DOI : 10.36106/ijsr

### *C. Comparison to the existing solutions*

In order to show the effectiveness of the proposed work, we compared it with most closely related and most recent studies Tavares [5] and Luis [23] in Table 5. Supervised learning algorithm random forest is used in the classification studies.

P.A. Tavares et al. [5] in their paper aimed to select the best LULC classification approach for tropical regions through random forest algorithm. The overall accuracy of 56.01% was obtained using S-1 data only. He suggested integration of S-1 and S-2 data to improve the classification accuracy.

Luis [23] exploited the use of metrics like mean and median from the satellite data over a period of time.

**Table 5. Comparison of proposed work with existing solutions**

| S. No | Parameters | Tavres [5] | Luis [23] | Proposed work |
|---|---|---|---|---|
| 1 | Area of Study | Tropical Area Belem, Brazil, Amazon | 82.7% of Wales & bordering region of England in UK | Bhiwani district in Haryana, India |
| 2 | Type of Sentinel-1 Image | SLC (Single looking Complex) | GRD (Ground Range Detected) Level-1 | GRD (Ground Range detected) Level-1 |
| 3 | Pre-processing Steps | Calibration, thermal noise removal, Terrain Correction | Calibration, Lee Speckle filter, Terrain Correction | Orbit file correction, calibration, Lee speckle noise removal, Terrain Correction |
| 4 | Machine learning Methods | Random Forest | Random Forest | Random Forest, KNN, Maximum Likelihood |
| 5 | Overall Accuracy (OA) | 56.01% for S-1 | 61% for S-1 interval 1, 2 | RF-62.5%, KNN-73% ML-68.23% for S-1 |

Land cover maps were created using temporal aggregation for over one year of data. Based on the classification using the random forest algorithm the overall accuracy (OA) of sentinel-1 images ranged from 61-69% based on time intervals. The OA increases with the increase in the number of time intervals (1, 2, 3, 4, 6, 12). The level of accuracy was recorded as 61% for interval 1, 2 and 69% for mean over 12 intervals.

The overall accuracy of classification for the proposed work is recorded as 62.5% for Sentinel-1 images using the random forest algorithm which is better as compared to the results given by Tavares [5](2019) & Luis [23](2019) for the interval 1, 2. The orbit file correction step was missing from the above studies. In the proposed work the importance of the orbit file correction step is highlighted as it has improved the classification results as compared to the above studies.

## 5. Conclusions & Future Work

In this paper, we contribute a useful set of pre-processing techniques of the Sentinel-1 images before using it for any kind of classification problem. The accuracy of classification is improved in the range of 1-15% after the removal of these errors from the image. This improvement can be visually seen in the KNN and random forest algorithms with 15% and 13.1% increase in the accuracy respectively. In comparison with KNN and RF, Maximum Likelihood algorithm observed an increase of only 1.03% in the classification accuracy. The orbit file correction has often not been applied in several studies, so an attempt has been made to study the impact of this step on the accuracy and the results are encouraging. A further increase of 1.52% in the overall accuracy can be recorded with this step along with others. The present paper provides a sincere effort to put all steps systematically and exhaustively which will be helpful for researchers working on various kinds of analysis involving the use of Sentinel-1 SAR images.

The future scope of this work is the integration of Sentinel-1 & Sentinel-2 images to improve the overall accuracy of classification. Other variables such as texture, S-2 indices, metrics like mean and median and SRTM must be exploited for better LULC mapping. More than one image for multiple dates must be taken to exploit the temporal advantage of sentinel-1 images.

## REFERENCES


[1] Kim, D. J., Hensley, S., Yun, S. H., & Neumann, M. (2016). Detection of durable and permanent changes in urban areas using multitemporal polarimetric UAVSAR data. *IEEE Geoscience and Remote Sensing Letters*, *13*(2), 267-271.

[2] Lee, J. S., Jurkevich, L., Dewaele, P., Wambacq, P., & Oosterlinck, A. (1994). Speckle filtering of synthetic aperture radar images: A review. *Remote sensing reviews*, *8*(4), 313-340.

[3] Lukin, V., Rubel, O., Kozhemiakin, R., Abramov, S., Shelestov, A., Lavreniuk, M., ... & Chehdi, K. (2018). Despeckling of multitemporal sentinel SAR images and its impact on agricultural area classification. *Recent Advances and Applications in Remote Sensing*, 21-40.

[4] Kaushik, P., & Jabin, S. (2018, December). A Comparative study of pre-processing techniques of SAR images. In *2018 4th International Conference on Computing Communication and Automation (ICCCA)* (pp. 1-4). IEEE.

[5] Tavares, P. A., Beltrão, N. E. S., Guimarães, U. S., & Teodoro, A. C. (2019). Integration of sentinel-1 and sentinel-2 for classification and LULC mapping in the urban area of Belém, eastern Brazilian Amazon. *Sensors*, *19*(5), 1140.

[6] Nyoungui, A. N., Tonye, E., & Akono, A. (2002). Evaluation of speckle filtering and texture analysis methods for land cover classification from SAR images. *International Journal of remote sensing*, *23*(9), 1895-1925.

[7] Mansourpour, M., Rajabi, M. A., & Blais, J. A. R. (2006, February). Effects and performance of speckle noise reduction filters on active radar and SAR images. In *Proc. ISPRS* (Vol. 36, No. 1, p. W41).

[8] Li, A., & Loffeld, O. (1991). Two dimensional SAR processing in the frequency domain. In *IGARSS'91; Proceedings of the 11th Annual International Geoscience and Remote Sensing Symposium* (Vol. 2, pp. 1065-1068).

[9] Zaugg, E. C., & Long, D. G. (2009). Generalized frequency-domain SAR processing. *IEEE Transactions on Geoscience and Remote Sensing*, *47*(11), 3761-3773.

[10] Ranjitha, S., & Hiremath, S. G. (2018). High Density Impulse Noise Removal and Edge Detection in SAR Images based on random forest classifier. in Journal of Advanced Research in Dynamical and Control Systems (pp. 2187-2197)

[11] Gao, Y., Zhang, S., Zhang, K., & Li, S. (2019). Frequency domain filtering SAR interferometric phase noise using the amended matrix pencil model. *Comput. Model. Eng. Sci.*, *119*(2), 349-363.

[12] Abdikan, S., Sanli, F. B., Ustuner, M., & Calò, F. (2014, February). Land cover mapping using sentinel-1 SAR data. In *The International Archives of the Photogrammetry, Remote Sensing and Spatial Information Sciences, Volume XLI-B7, 2016 XXIII ISPRS Congress*.

[13] Fonteh, M. L., Theophile, F., Cornelius, M. L., Main, R., Ramoelo, A., & Cho, M. A. (2016). Assessing the utility of Sentinel-1 C band synthetic aperture radar imagery for land use land cover classification in a tropical coastal systems when compared with Landsat 8. *Journal of Geographic Information System*, *8*(04), 495.

[14] Borah, S. B., Sivasankar, T., Ramya, M. N. S., & Raju, P. L. N. (2018). Flood inundation mapping and monitoring in Kaziranga National Park, Assam using Sentinel-1 SAR data. *Environmental monitoring and assessment*, *190*(9), 1-11.

[15] Amitrano, D., Di Martino, G., Iodice, A., Riccio, D., & Ruello, G. (2018). Unsupervised rapid flood mapping using Sentinel-1 GRD SAR images. *IEEE Transactions on Geoscience and Remote Sensing*, *56*(6), 3290-3299.

[16] Liu, C. H. A. N. G. (2016). *Analysis of Sentinel-1 SAR data for mapping standing water in the Twente region* (Master's thesis, University of Twente).

[17] Twele, A., Cao, W., Plank, S., & Martinis, S. (2016). Sentinel-1-based flood mapping: a fully automated processing chain. *International Journal of Remote Sensing*, *37*(13), 2990-3004.

[18] Boni, G., Ferraris, L., Pulvirenti, L., Squicciarino, G., Pierdicca, N., Candela, L., ... & Pagliara, P. (2016). A prototype system for flood monitoring based on flood forecast combined with COSMO-SkyMed and Sentinel-1 data. *IEEE Journal of Selected Topics in Applied Earth Observations and Remote Sensing*, *9*(6), 2794-2805.

[19] European Space Agency Copernicus Open Access Hub. https://scihub.copernicus.eu/ . Online accessed on date March 14, 2020

[20] European Space Agency Terms and Conditions. https://scihub.copernicus.eu/twiki/do/view/SciHubWebPortal/TermsConditions. Accessed on Date March 14,2020

[21] European Space Agency STEP: Science toolbox exploitation Platform. https://step.esa.int/main/toolboxes/snap/. Accessed on March 14, 2020

[22] Filipponi, F. (2019). Sentinel-1 GRD preprocessing workflow. In *Multidisciplinary Digital Publishing Institute Proceedings* (Vol. 18, No. 1, p. 11).

[23] Carrasco, L., O'Neil, A. W., Morton, R. D., & Rowland, C. S. (2019). Evaluating combinations of temporally aggregated Sentinel-1, Sentinel-2 and Landsat 8 for land cover mapping with Google Earth Engine. *Remote Sensing*, *11*(3), 288.

[24] Mishra, S., & Jabin, S. (2020, October). Land Use Land Cover Change Detection using LANDSAT images: A Case Study. In *2020 IEEE 5th International Conference on Computing Communication and Automation (ICCCA)* (pp. 730-735). IEEE.

[25] Kaushik, P., & Jabin, S. (2021). Deforestation Mapping Using MODIS Tree Cover Mask and Sentinel-1 Images. In *Micro-Electronics and Telecommunication Engineering* (pp. 73-80). Springer, Singapore.


**FOOTNOTES**

- https://scihub.copernicus.eu/dhus/odata/v1/Products('a0f37c61-0211-45ac-b5c8-90f8fac045cf')/$value
- https://scihub.copernicus.eu/dhus/odata/v1/Products('5b96553b-b08b-4c20-9b45-88269a16251a')/$value